9th INTERNATIONAL SYMPOSIUM ON MEASURMENT AND QUALITY CONTROL (9th ISMQC)
November 21 - 24, 2007, IIT Madras

CALIBRATION OF 6 DOF PARALLEL MECHANISM DRIVEN BY PLANAR MOTORS

Kiyoshi Takamasu, Keisuke Yoshida, Tatsuya Senoo, Xin Chen, Kiyoshi Kotani and Satoru Takahashi
Department of Precision Engineering, The University of Tokyo
7-3-1, Hongo, Bunkyo-ku Tokyo, 113-8656 JAPAN
E-mail: takamasu@pe.t.u-tokyo.ac.jp

Abstract: *For high flexibility of assembly works, 6 DOF mechanisms are useful for supporting assembly workers. The 6 DOF mechanism needs to move in sub-mm and sub-degree absolute positioning accuracy over wide working area. For this purpose, we developed a novel 6 DOF parallel mechanism driven by 3 planar motors and a novel calibration method for this mechanism. The calibration experiments using CMM are performed and the results of the calibrations are evaluated.*
Key words: *Parallel mechanism, planar motor, kinematic calibration, CMM, uncertainty evaluation*

1. INTRODUCTION

For high flexibility of assembly works, we proposed AWB (Attentive Workbench) which is an intelligent cell production system. Fig. 1 shows a schematic view of attentive workbench. 6 DOF mechanisms are useful for supporting assembly workers in AWB. The 6 DOF mechanism needs to move in sub-mm of translation and sub-degree of rotation for absolute positioning accuracy over wide working area. For this purpose, we developed a novel 6 DOF parallel mechanism driven by 3 planar motors (Chen et al., 2004) (Kuhlbusch et al., 1999) (Kuchel 2001).

Fig. 2 shows the construction of the proposed parallel mechanism. When the planar motors are adapted to the mechanism, the working area of translation in X axis and Y axis, and the angular range on Z axis of the table are only limited by the size of working surface and the working range of the wires of control and power to the planar motors. Fig. 3 shows the variations of angular and Z position of the mechanism. These variations indicate ability of the wide working area of the mechanism.

When we use these type mechanisms in industry, the kinematic calibration method is key technology to control the position and angle precisely. The kinematic calibration for 6 DOF and three dimensional mechanisms are difficult in the calculation methods and also three dimensional measurement methods (Bai & Teo, 2003) (Ben-Horin et al., 1998). For the calibration, we developed a novel calibration method for this mechanism using the calibration method for 3 DOF parallel mechanism with CMM (coordinate measuring machine) (Sato et al., 2002).

Fig. 1 Schematic view of attentive workbench (AWB)

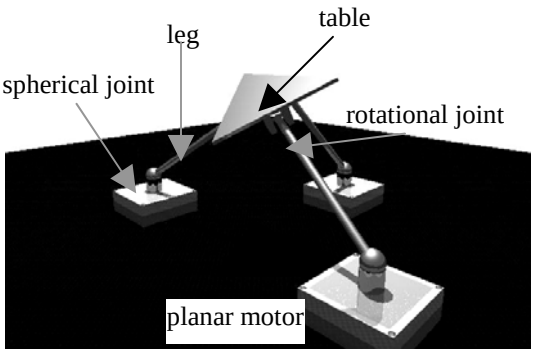

Fig. 2. Construction of 6 DOF parallel mechanism driven by 3 planar motors.

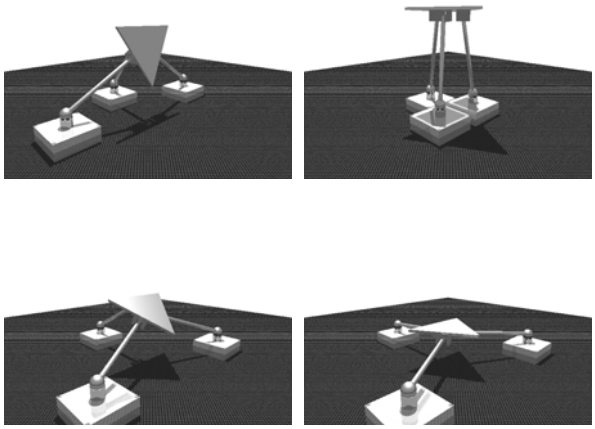

Fig. 3. Variations of angular position and Z position of 6 DOF parallel mechanism.

2. KINEMATIC PARAMETERS OF 6 DOF PARALLEL MECHANISM

Table 1 shows the list of kinematic parameters of the 6 DOF parallel mechanism (see Fig. 4). The table has 9 parameters for positions of the three rotational joints and 9 parameters for angular directions of the rotational joints. The three trays have 9 parameters of offsets of three spherical joints.

Table 1. Kinematic parameters of the 6 DOF parallel mechanism

positions of rotational joints 1, 2, and 3 on the table	rx_1, ry_1, rz_1 rx_2, ry_2, rz_2 rx_3, ry_3, rz_3
axis directions of rotational joints 1, 2, and 3 on the table	sx_1, sy_1, sz_1 sx_2, sy_2, sz_2 sx_3, sy_3, sz_3
lengths of legs 1, 2, and 3	w_1, w_2, w_3
offsets of spherical joints 1, 2, and 3 on the tray 1, 2, and 3	bx_1, by_1, bz_1 bx_2, by_2, bz_2 bx_3, by_3, bz_3

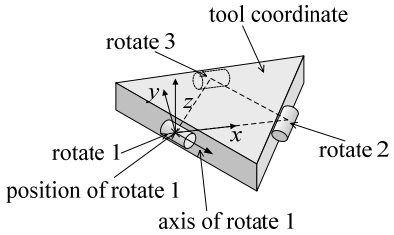

(a) parameters on the table

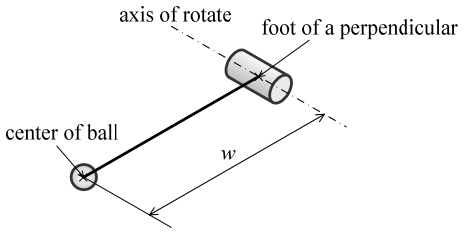

(b) Parameter on the leg

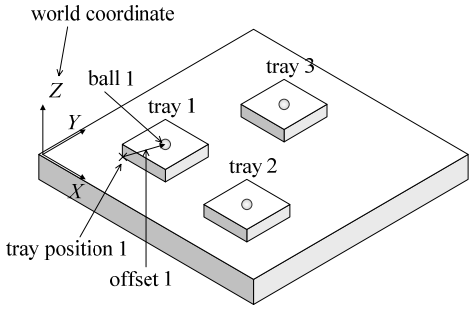

(c) parameters on the planar motor (tray 1, 2, and 3)

Fig. 4. Schematic of the kinematic parameters for 6 DOF parallel mechanism

Total number of the kinematic parameters is 27, because only six out of nine parameters for direction of rotational joints are independent.

3. REVERSE AND FORWARD KINEMATICS

The reverse kinematics that calculates the positions of the planar motors from position and angle of the table is solved analytically. To simplify the analytical solution, we assumed the simplified model that described under the assumptions of Fig. 5. The input and output parameters of the reverse kinematics on the simplified model are shown in Table 2.

Table 2. Input and output parameters of the reverse kinematics on the simplified model

input	position of the table	X, Y, Z
input	angle of the table	tx, ty, tz
output	position of the tray 1, 2, and 3	qx_1, qy_1 qx_2, qy_2 qx_3, qy_3

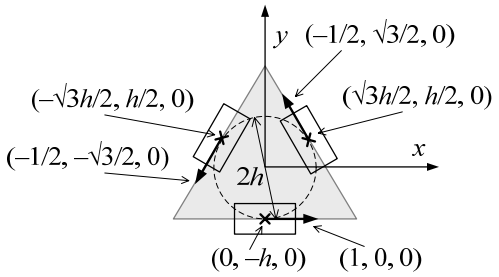

Fig. 5. Assumptions of parameters, 9 positions and 9 directions of the 3 rotational joints on the table are defined at ideal positions and directions for simplified model.

Fig. 6 illustrates the calculation method for the reverse kinematics, when the table position (X, Y, Z) is assumed (0, 0, uz). The length wr are calculated from the position Z axis uz, offset of Z axis bz, and length of leg w. Then, lengths wx and wy are calculated from the rotational angle of the table sb according to the equations (1), (2), and (3). From wx and wy, the two dimensional position of the tray is calculated, where bz is Z offset of the tray and sb is angle of the table.

Using the reverse kinematics and Newton method, the forward kinematics is solved numerically. The solutions of the reverse and forward kinematics allow for evaluating the working area of the table. Fig. 7 illustrates the example of the working area analysis. The angular range on X axis and Y axis of the table is found the illustrated area when length of legs w is 100 mm and radius of the table h is 20 mm. The large angular working area tx and ty can be achieved over ±60 degree in the

reverse and forward kinematics analysis.

$$wr = \sqrt{w^2 - (uz - bz)^2} \quad (1)$$

$$wx = (uz - bz)\tan sb \quad (2)$$

$$wy = \pm\sqrt{wr^2 - wx^2} \quad (3)$$

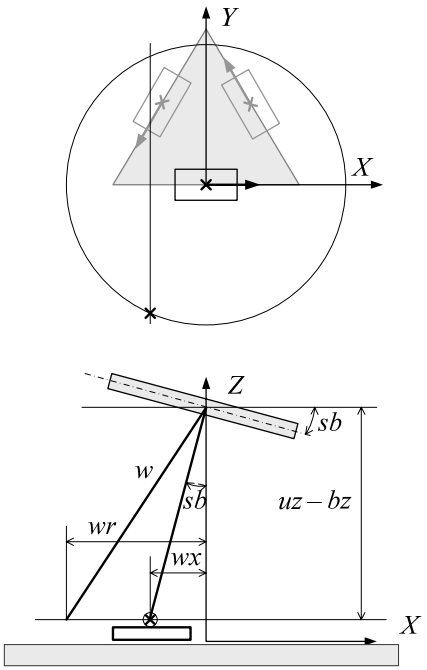

Fig. 6. Calculation method is defined for the reverse kinematics. Tray position *wx* is calculated from Z position *uz* and angle *sb* of the table.

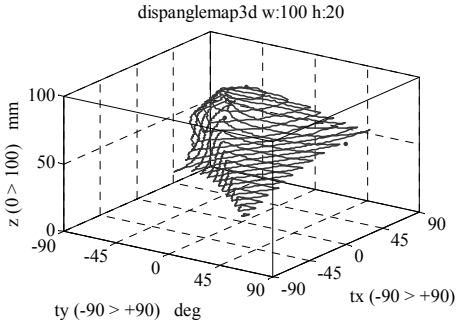

Fig. 7. Angular range on X axis and Y axis of the table; length of legs: 100 mm, radius of table: 20 mm.

4. PROTOTYPE OF 6 DOF PARALLEL MECHANISM

We made a prototype of the mechanism shown in Fig. 8 (Chen et al., 2004). The main parameters of the mechanism are length of legs *w* 83 mm and radius of the table *h* 30 mm.

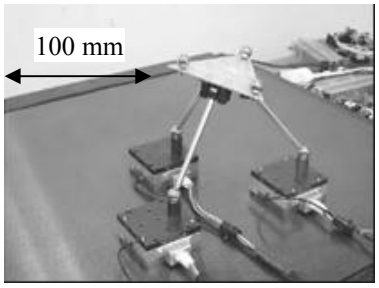

Fig. 8. Prototype of 6 DOF parallel mechanism

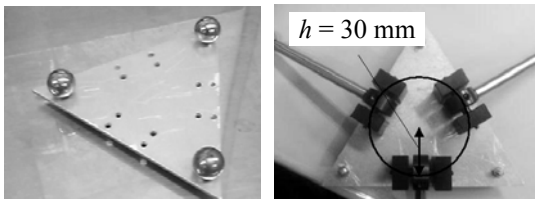

(a) Table

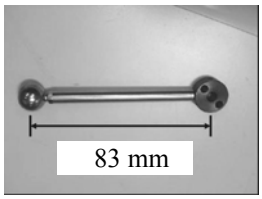

(b) Leg

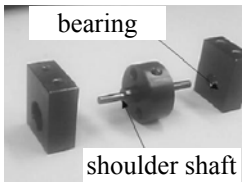

(c) Rotational joint

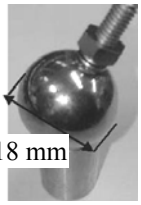

(d) Spherical joint

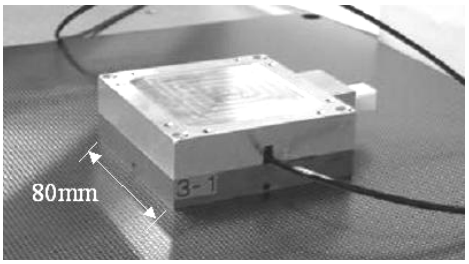

(e) Tray: Sawyer type planar motor

Fig. 9. Mechanical parts of the prototype

Fig. 9 shows a table, a leg, a rotational joint, a spherical joint, and a tray. The table has 3 balls on the top size for measuring position and angle of the table and 3 rotational joints on the back side (Fig. 9 (a)). The length of the leg is 83 mm (Fig. 9 (b)). The rotational joint consists of the rotational bearings and a shoulder shaft (Fig. 9 (c)). The spherical joint is a magnet type and has

the ball of 18 mm diameter (Fig. 9 (d)). The trays are the planar motors by Sawyer type stepping motors (Sawyer, 1969) (Fig. 7 (e)); the size of the motor is 80 mm×80 mm×28 mm and resolution of a step is 42 μm, repeatability is 3 μm and absolute accuracy is 23 μm.

The total size of the prototype of 6 DOF parallel mechanism is approximately 200 mm×200 mm×150 mm. The size of the platen (surface of movement for the trays) is 500 mm×500 mm. Fig. 10 illustrates large angle position of the prototype. The Large angular working area of the maximum angle on X axis is over 70 deg can be achieved by the prototype.

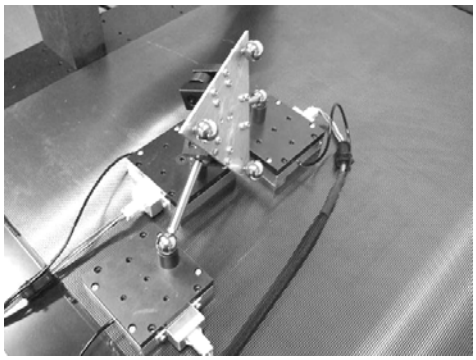

(a) Photograph when the table at maximum angle

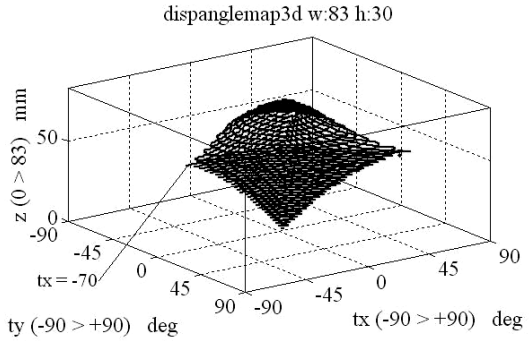

(b) Angular range on X axis and Y axis of the table

Fig. 10. Large angular working area of maximum angle on X axis is over 70 deg, when length of leg w is 83 mm and radius of the table h is 30 mm.

5. CALIBRATION METHOD

When the 6 DOF mechanisms are use to support assembly works, the absolutely calibration of all kinematic parameters of the mechanism are essential for the accurate positioning of the mechanisms (Hollerbach & Lokhorst, 1995) (Khalil & Besnard, 1999). Total number of the kinematic parameters is 27, such as positions and direcitions of the rotational joints, offsets of the spherical joints and so on. We solve the least square method to calculate the values of parameters using the the forward kinematics and Newton method (Sato et al., 2002) (Sato et al., 2004) (Zhuang, 1997).

Equation (4) shows the forward kinematics **f**, where *X*, *Y*, *Z* and *tx*, *ty*, *tz* are positions and angles of the table when **x** is positions of the trays and the parameters **P** are applied. The relationship of the positional errors of the trays *d***x** and the parameter errors *d***P** is indicated as equation (5). The ratio $\Delta\mathbf{f}/\Delta P_i$ is calculated numerically. Therefore, the values of the parameter errors *d***P** can be calculated using equation (5).

$$^{t}(X, Y, Z, tx, ty, tz) = \mathbf{f}(\mathbf{x}, \mathbf{P}) \tag{4}$$

$$d\mathbf{x} = \sum_{i=1}^{n} \frac{\Delta\mathbf{f}}{\Delta P_i} dP_i \tag{5}$$

In these equations, parameters **P** is (P_1, P_2, ⋯, P_n), and the position of the tray **x** is (x_1, y_1, x_2, y_2, x_3, y_3). The positional errors of the table in k times measurement $\mathbf{E}_x$ is defined as equation (6) and the parameter errors $\mathbf{E}_p$ is defined as equation (7).

$\mathbf{E}_p$ is calculated by equation (8) using the least squares method, where $\mathbf{J}_p$ is Jacobian matrix of the forward kinematics (see equation (9)) and **W** is error matrix of measurements (see equation (10)) from measuring errors of the position of the trays, the positions, and angles of the table.

$$\mathbf{E}_x = \begin{bmatrix} d\mathbf{x}_1 & d\mathbf{x}_2 & \cdots & d\mathbf{x}_k \end{bmatrix}^T \tag{6}$$

$$\mathbf{E}_P = \begin{bmatrix} dP_1 & dP_2 & \cdots & dP_n \end{bmatrix}^T \tag{7}$$

$$\mathbf{E}_P = (\mathbf{J}_p^t \mathbf{W}^{-1} \mathbf{J}_p)^{-1} \mathbf{J}_p^t \mathbf{W}^{-1} \mathbf{E}_x \tag{8}$$

$$\mathbf{J}_p = \begin{pmatrix} \frac{\Delta\mathbf{f}(\mathbf{x}_1, \mathbf{P})}{\Delta P_1} & \cdots & \frac{\Delta\mathbf{f}(\mathbf{x}_1, \mathbf{P})}{\Delta P_n} \\ \vdots & \ddots & \vdots \\ \frac{\Delta\mathbf{f}(\mathbf{x}_k, \mathbf{P})}{\Delta P_1} & \cdots & \frac{\Delta\mathbf{f}(\mathbf{x}_k, \mathbf{P})}{\Delta P_n} \end{pmatrix} \tag{9}$$

$$\mathbf{W} = \begin{pmatrix} \mathbf{W}_1 & & & \mathbf{0} \\ & \mathbf{W}_2 & & \\ & & \mathbf{W}_3 & \\ & & & \ddots \\ \mathbf{0} & & & \mathbf{W}_k \end{pmatrix} \tag{10}$$

After the calibration, the uncertainties of the parameters $\mathbf{E}_p$ are evaluated according to equation (11). Where **C** is a diagonal matrix of eigen values. The uncertainties of the parameters are influenced by the eigen values of the diagonal matrix **C** in equation (12). The condition number of matrix **C**; the ratio of the maximum λ_{max} and the minimum λ_{min} of eigen values will be effected by the positions and angles of the measurements of the calibration. Table 3 shows the relationship of the ratio of eigen values and the positions and angles of the calibrations. The wide range of positions and angles in the calibrations has the small condition number.

$$\mathbf{E}_p = \mathbf{Q}^{-1}\mathbf{C}\mathbf{Q} \tag{11}$$

$$\mathbf{C} = \begin{pmatrix} \lambda_1 & 0 & 0 & 0 \\ 0 & \lambda_2 & 0 & 0 \\ 0 & 0 & \ddots & 0 \\ 0 & 0 & 0 & \lambda_n \end{pmatrix} \quad (12)$$

Table 3. Relationship between range of angle of the table in the calibration and the condition number (eigen value ratio) of diagonal matrix **C**.

calibration pattern	pattern a	pattern b	pattern c
angle range	wide	1/2 of pattern a	small
condition number of **C**; ratio of $\lambda_{max}/\lambda_{min}$	1.8×10^3	2.2×10^3	3.4×10^6

6. CALIBRATION EXPERIMENTS

Using this calibration method, we calibrated the mechanism measured by CMM (coordinate measuring machine) shown in Fig. 11. For measurements by CMM, three target spheres are mounted on the table shown in Fig. 12. Before the calibration, the offsets of spherical joints 1, 2, and 3 on the trays 1, 2, and 3 are measured by CMM in Fig. 13. Fig. 14 shows measurements of positions and angles of the table by CMM using three target spheres for the calibration.

The variation of attitudes of the table in the calibration effects the result of calibration. Table 4 shows the relationship between the condition number of the diagonal matrix **C** and the average residuals of positions of the table. This result indicates that the condition number relates to the calibration accuracy.

The absolute accuracy of the calibration is evaluated from measurement of the position of an additional sphere on the table by an optical position sensor shown in Fig. 15 (Usuki et al., 2004). Fig. 16 illustrates the positions of the sphere on the table in variable attitudes of the table for before and after the calibration. The absolute accuracy of the table is approximately 0.509 mm after the calibration with the compensation of effect by the center of gravity. Therefore, we confirm that the proposed 6 DOF parallel mechanism and the calibration method is applicable for assembly works in AWB.

Table 4. Relationship between the condition number of matrix **C** and the average residuals of positions of the table

attitude pattern of the table in the calibration	narrow	wide
condition number of matrix **C**	6.0446×10^6	9.3746×10^3
average residuals of positions of the table	0.203 mm	0.038 mm

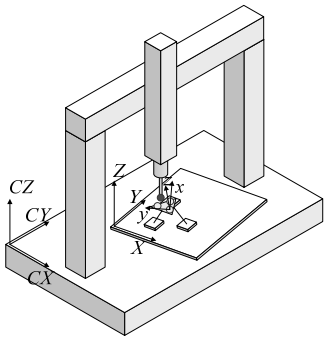

Fig. 11. Calibration experiments are performed by measurements of the positions of table by CMM (Coordinate Measuring Machine). *CX*, *CY* and *CZ* is coordinate system of CMM.

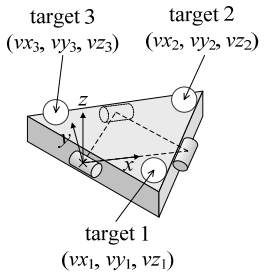

Fig. 12. Three target spheres on the table for measurement of position and angle of the table.

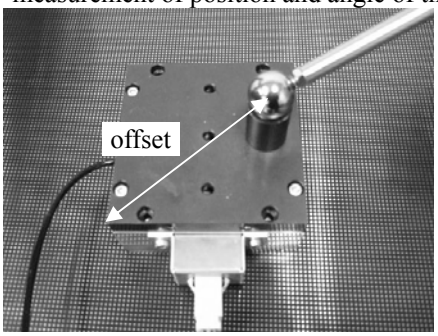

Fig. 13. Offset of spherical joints of the tray.

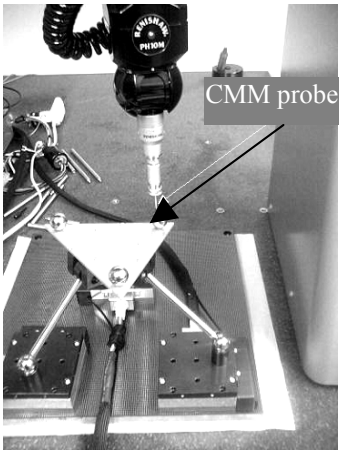

Fig. 14. Measurement of position and angle of the table by CMM for the calibration

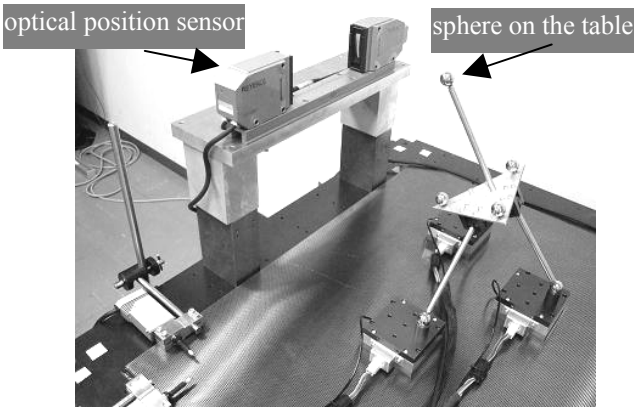

Fig. 15. Evaluation of absolute accuracy of the table after calibration by an optical position sensor

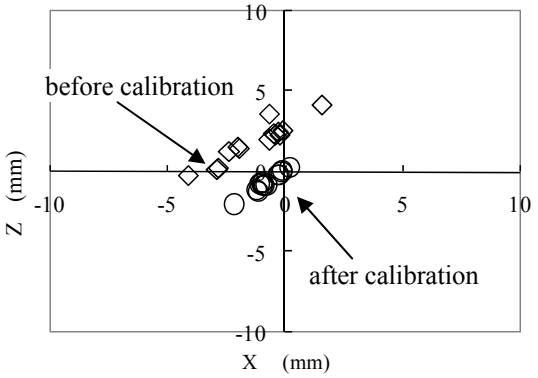

Fig. 16. Positions of the sphere on the table in variable attitudes of the table for before and after the calibration

7. CONCLUSIONS

For high flexibility of assembly works, 6 DOF mechanisms are useful for supporting assembly workers in AWB. We developed a novel 6 DOF parallel mechanism driven by 3 planar motors. The kinematic calibrations for 6 DOF three dimensional mechanisms are difficult in the calculation methods and also three dimensional measurement methods. For the calibration, we developed a novel calibration method for this mechanism and performed the calibration experiments of the prototype mechanism. The absolute accuracy of the table is approximately 0.509 mm after the calibration. Therefore, we confirm that the proposed 6 DOF parallel mechanism and the calibration method is applicable for assembly works in AWB.

8. REFERENCES

Bai, S. & Teo, M. (2003). Kinematic calibration and pose measurement of a medical parallel manipulator by optical position sensors, *Journal of Robotic Systems*, Vol. 20, No. 4, pp. 201-209.

Ben-Horin, R.; Shoham, M. & Djerassi, S. (1998). Kinematics, dynamics and construction of a planarly acutuated parallel robot, *Robotics and Computer-Integrated Manuf.,* Vol. 14, pp. 163-172

Chen, X.; Kotani, K.; Takahashi, S. & Takamasu, K. (2004). Development of multiple small linear planar motor system, *Int. Conf. of the European Society for Precision Engg. and Nanotechnology*, pp. 252-253.

Hollerbach, J. & Lokhorst, D. (1995). Closed-loop kinematic calibration of the RSI 6-DOF hand controller, *IEEE Transactions on Robotics and Automation*, Vol. 11, No. 3, pp. 352-359.

Khalil, W. & Besnard, S. (1999). Self Calibration of Stewart-Gough Parallel Robots Without Extra Sensors, *IEEE Transactions on Robotics and Automation*, Vol. 15, No.6, 1116-1121

Kuhlbusch, W.; Moritz, W.; Luckel, J.; Toepper, S. & Scharfeld, F. (1999). TRIPLANAR − A New Process-Machine Type Developed by Means of the Mechatronics Design, *IEEE/ASME international Conference on Advanced Intelligent Mechatronics*, 514-519

Luckel, J. (2001). Iterative Model-based Design of Parallel Robot, TRIPLANAR, *IEEE/ASME international Conference on Advanced Intelligent Mechatronics*, 135-140

Sato, O.; Ishikawa, H.; Hiraki, M. & Takamasu, K. (2002). The Calibration of Parallel-CMM: Parallel-Coordinate Measuring Machine, *International Conference of the European Society for Precision Engineering and Nanotechnology*, 573-576

Sato, O.; Shimojima, K.; Furutani, R. & Takamasu, K. (2004). Artifact calibration of parallel mechanism, kinematic calibration with a priori knowledge, *Measurement Science and Technology*, 15(6), 1158-1165

Sawyer, B. (1969). Magnetic positioning device, *US Patent*, 3,457,482

Usuki, S.; Enami, K.; Sato, O.; Takahashi, S. & Takamasu, K. (2004). Improving the Accuracy of 3D Displacement Measurement using Ring-Shaped Laser Beam and High Resolution CCD, *International Conference of the European Society for Precision Engineering and Nanotechnology*, 328-329

Zhuang, H. (1997). Self-Calibration of Parallel Mechanisms with a Case Study on Stewart Platforms, *IEEE Transactions on Robotics and Automation*, Vol. 13, No. 3, 387- 397.